

# Imatinib ameliorates bronchiolitis obliterans via inhibition of fibrocyte migration and differentiation

著者	渡辺 知志
著者別表示	Watanabe Satoshi
journal or publication title	博士論文本文Full
学位授与番号	13301甲第4455号
学位名	博士（医学）
学位授与年月日	2016-09-26
URL	<a href="http://hdl.handle.net/2297/46465">http://hdl.handle.net/2297/46465</a>



IMATINIB AMELIORATES BRONCHIOLITIS OBLITERANS VIA INHIBITION OF FIBROCYTE  
MIGRATION AND DIFFERENTIATION

Satoshi Watanabe, MD<sup>1</sup>, Kazuo Kasahara, MD, PhD<sup>1</sup>, Yuko Waseda, MD, PhD<sup>1</sup>, Hazuki Takato, MD,  
PhD<sup>1</sup>, Shingo Nishikawa, MD<sup>1</sup>, Taro Yoneda, MD<sup>1</sup>, Johsuke Hara, MD, PhD<sup>1</sup>, Takashi Sone, MD,  
PhD<sup>1</sup>, Miki Abo, MD, PhD<sup>1</sup>, Hideharu Kimura, MD, PhD<sup>1</sup>, Shinji Nakao, MD, PhD<sup>2</sup>

<sup>1</sup>Department of Respiratory Medicine, Cellular Transplantation Biology, Kanazawa University  
Graduate School of Medical Sciences, Kanazawa, Japan

<sup>2</sup>Department of Hematology, Cellular Transplantation Biology, Kanazawa University Graduate School  
of Medical Sciences, Kanazawa, Japan

**Corresponding Author:** Satoshi Watanabe, MD

Department of Respiratory Medicine, Cellular Transplantation Biology, Kanazawa University Graduate  
School of Medical Sciences, 13-1, Takara-machi, Kanazawa #920-8641, Japan.

Tel : +81-76-265-2271, Fax : +81-76-234-4252, E-mail: swatanabe@staff.kanazawa-u.ac.jp

## **ABSTRACT**

**Background:** Imatinib, a tyrosine kinase inhibitor, has been proposed as a potential antifibrotic agent for fibroproliferative diseases, including bronchiolitis obliterans (BO). However, the underlying antifibrotic mechanisms of the agent remain unclear. We evaluated whether bone marrow-derived progenitor cells, fibrocytes, might be a target of imatinib in the attenuation of BO.

**Methods:** We used a murine BO model induced by heterotopic tracheal transplantation, and assessed the origin of fibroblasts by using GFP-bone marrow (BM) chimeric mice. We also evaluated the effects of imatinib on luminal obstruction and fibrocyte accumulation. Additionally, the effects of imatinib on fibrocyte migration and differentiation were assessed by culturing fibrocytes *in vitro*.

**Results:** In the murine BO model, tracheal allografts showed epithelial injury and developed complete luminal occlusion 28 days after transplantation. Most of the mesenchymal cells that had accumulated in the tracheal allograft were derived from BM cells. Imatinib treatment ameliorated the airway luminal occlusion and significantly reduced the number of fibrocytes in the allografts. *In vitro* studies showed that imatinib inhibited migration of cultured blood fibrocytes via the PDGF/PDGFR axis. Additionally, imatinib inhibited differentiation of fibrocytes via suppression of c-Abl activity that was essential for the differentiation of monocytes to fibrocytes.

**Conclusions:** Imatinib prevents airway luminal obstruction by inhibiting the migration and differentiation of fibrocytes. Fibrocytes may be a novel target in the prevention and treatment of BO.

## **INTRODUCTION**

Bronchiolitis obliterans (BO) is a fibroproliferative disorder resulting in terminal small airway occlusion that leads to an irreversible decline in lung function (1). BO occurs in more than 50% of lung transplant recipients within 5 years of lung transplantation, and it remains the predominant cause of morbidity and mortality following lung transplantation (2). BO responds poorly to corticosteroids or immunosuppressants. Lung transplant physicians and respirologists need to elucidate its pathogenesis and identify useful biomarkers for the diagnosis and severity of BO as well as effective interventions to prevent and treat BO.

Imatinib is a tyrosine kinase inhibitor of Bcr-Abl, c-Abl, c-Kit, and PDGFR (3). Recent preclinical and clinical studies have suggested that imatinib is effective for the treatment of fibroproliferative disorders such as pulmonary fibrosis, lupus nephritis and pulmonary hypertension (4-8). We previously reported two cases of BO after allogeneic hematopoietic stem cell transplantation that were successfully treated with imatinib (9). In the two cases, imatinib treatment stabilized the patients' pulmonary function and prolonged their survival time. Several studies have also described the efficacy of imatinib in the treatment of BO in patients with chronic graft-versus-host disease (10-12). In the rat BO model of heterotopic tracheal transplantation (HTT), imatinib inhibited the tracheal luminal occlusion 30 days after transplantation compared with vehicle-treated allografts (13, 14). Taken together, these data suggest that imatinib can be a useful agent for treating BO.

The precise mechanisms by which imatinib ameliorates BO are incompletely understood. In the

rat BO model, imatinib inhibited the development of luminal occlusions without suppressing inflammatory cells, suggesting direct anti-fibrotic effects of imatinib (13). On the other hand, late administration of imatinib during the fibroproliferative phase of BO failed to prevent luminal obstruction (14). These findings suggest that imatinib exerts its preventative effects on fibroproliferative lesion development in tracheal allografts only when it is administered during the inflammatory phase of BO; and that the therapeutic target of imatinib may exist soon after tracheal transplantation.

One of the cellular components that is involved in the fibroproliferative lesion is a bone marrow (BM)-derived mesenchymal progenitor cell, the fibrocyte. Fibrocytes represent 0.1–0.5% of the circulating leukocytes that differentiate from monocyte precursors and co-express the leukocyte marker CD45 and mesenchymal markers such as collagen I (15). Fibrocytes act as precursors of fibroblasts that participate in tissue remodeling and also the secretion of inflammatory cytokines, chemokines, and growth factors that contribute to the pathogenesis of fibrotic disorders (16-18). In lung tissue from BO patients who underwent lung transplantation, increased numbers of fibrocytes are identified in the alveolar parenchyma (19). The number of peripherally circulating fibrocytes was also increased with advancing BO stage, suggesting that fibrocytes may play an important profibrotic role in the development of BO (20).

We hypothesized that in the BO model of HTT, imatinib ameliorated BO by inhibiting fibrocytes via unknown mechanisms. To test this hypothesis, we examined the causal role of fibrocytes in the development of BO by using GFP-chimeric mice. In this model, we evaluated the effect of imatinib on

the airway obstruction of transplanted tracheas as well as the effect on fibrocytes *in vivo*. Furthermore, to investigate the mechanisms underlying fibrocyte regulation by imatinib, we conducted an *in vitro* assessment of the targets of imatinib, i.e., c-Abl, c-Kit and PDGFR.

## **METHODS**

### **Murine BO Model**

Animal studies were approved by the Institute for Experimental Animals, Kanazawa University Advanced Science Research Center. Male 7- to 10-week-old BALB/c, C57BL/6 wild-type mice, and GFP-positive transgenic (GFP-Tg) mice on a C57BL/6 background were purchased from Sankyo Laboratory Service Corporation (Toyama, Japan). The heterotopic tracheal transplantation (HTT) model was prepared as previously described (21, 22). A trachea from a BALB/c (isograft) or a C57BL/6 (allograft) was transplanted into a BALB/c mouse. Imatinib was kindly provided by Novartis (Basel, Switzerland). This solution was diluted with 0.9% saline and injected intraperitoneally once daily (final dosage, 10 mg/kg/day). GFP-BM chimeras in which BM was replaced by GFP-marked BM cells were also prepared as previously described (23). The heterotopic tracheal transplantation was performed 2 months after BM transplantation. Allogenic HTT was performed by transplanting tracheas from BALB/c to GFP-Tg, GFP-Tg to BALB/c and BALB/c to GFP-BM chimeras. Transplanted grafts were isolated on the indicated days after transplantation. Tracheal tissues were washed in phosphate-buffered saline (PBS), fixed in 10% formaldehyde and embedded in paraffin, or embedded directly in Tissue-

Tek OCT compound (Sakura, Alphen aan den Rijn, The Netherlands) and snap-frozen in liquid nitrogen.

Frozen tissues were serially cut into 14- $\mu$ m thick cross-sections and stored at -80°C until used.

### **Histopathological Analysis**

Tracheal graft sections were stained with hematoxylin and eosin. The degree of airway injury and luminal occlusion was examined as previously described (21). Evaluations used the NIH Image J program, version 1.49 p (National Institutes of Health. National Technical Information Service, Springfield, VA).

### **Culturing Murine or Human Fibrocytes**

Human peripheral blood was collected from healthy adult volunteers after informed consent was obtained under the guidance of the ethical committee of Kanazawa University Graduate School of Medicine. Fibrocytes were harvested and cultured as previously described (24, 25). Briefly, peripheral blood mononuclear cells (PBMCs) were isolated from murine or human blood by using Lymphoprep™ (Progen Biotechnik). Human monocytes were isolated using a Dynabeads® FlowComp™ Human CD14 Kit (Life technologies). We prepared serum-free medium that consisted of RPMI 1640, 1% non-essential amino acid, 1% pyruvate, 1% ITS-3, and 1% penicillin and streptomycin. We also prepared serum-containing medium consisting of DMEM, 10% heat-inactivated human AB serum (Sigma Aldrich), and penicillin/streptomycin. PBMCs or CD14-positive cells were cultured in 96-well plastic

plates or 8-well glass slides.

### **Immunostaining**

Paraffin-embedded tissues were incubated with rabbit anti-GFP antibody in the experiments using GFP chimeric mice. Frozen tissues/cells were fixed in 4% paraformaldehyde, blocked with 2% skim milk in 0.2% Triton X-100/PBS and were then stained with the primary antibodies. These sections were stained using specific antibodies followed by appropriate secondary antibodies and Hoechst 33342. The inflammatory cells observed in sections were expressed as the number of positively-staining cells per tracheal graft cross-section in 10 separate, high-power ( $\times 400$ ) fields. The densities of endothelial cells and pericytes were defined as the percent of pixels covered by each individual staining marker. The cellular localization of fluorescently labeled proteins was viewed under fluorescent microscopy (Zeiss). The details of the antibodies are provided in the online supplement.

### **Phenotype, Migration and Differentiation of Fibrocytes**

We examined the protein expression of c-Abl, PDGFR $\alpha$ , PDGFR $\beta$ , and c-Kit by murine or human fibrocytes by using immunofluorescence or flow cytometry. Migration of fibrocytes was assessed by using Boyden chambers coated with collagen I, as previously described (26, 27). Recombinant human PDGF-AA, PDGF-BB, and SCF were used as the chemoattractants. Differentiation of fibrocytes was assessed as previously described (28). Imatinib or other inhibitors such as nilotinib (c-Abl inhibitor),



crenolanib (PDGFR inhibitor), or masatinib (c-Kit inhibitor) (Selleck Chemicals, Japan) were used at the appropriate concentrations. Additional details are provided in the online supplement.

### **Transfection Experiment**

Human PBMCs were isolated and purified as described above. PBMCs were transfected with ABL1 Silencer select siRNAs or control siRNAs (Applied Biosystems/Ambion, Austin, TX, USA) using Lipofectamine 2000 (Invitrogen) according to the manufacturer's instructions. After 5 days of culturing, the ratio of fibrocytes to total cells was determined by microscopic examination.

### **Statistical Analysis**

Data are expressed as means  $\pm$  SEM. Statistical analyses were performed using the Mann-Whitney U test. A P value less than 0.05 was considered to indicate statistical significance. All data were analyzed with IBM SPSS Statistics for Windows, version 22.

## **RESULTS**

### **Imatinib attenuated luminal obstruction in the tracheal allograft**

In the BO model of HTT, the isografts showed epithelial injury soon after transplant, but recovery from injury was rapid and there was no evidence of luminal occlusion. On the other hand, the allografts

showed rapid development of severe epithelial injury that persisted. The lumens of the trachea gradually filled with fibroproliferative lesions leading to luminal occlusion by day 28 (Figure 1A and 1B).

We next examined the effects of imatinib on the tracheal allografts, again using the HTT model. Recipients of allografts were treated daily with 10 mg/kg imatinib (prophylaxis) or a control (vehicle) from days 1 to 28 and were evaluated 28 days after transplantation. We also examined imatinib treatment administered to the allograft recipients from days 1 to 14 (early treatment) or from days 15 to 28 (late treatment) (Figure 1C). The allografts of the recipients that were treated prophylactically with imatinib showed significantly reduced luminal occlusion in comparison with the allografts treated with vehicles ( $P < 0.05$ ). However, early treatment as well as late treatment failed to inhibit the airway obstruction after 28 days (Figure 1D). Although prophylaxis showed significantly less luminal obliteration than that in late treatment, there were no statistically significant differences between prophylaxis and early treatment. These findings indicated that continuous administration of imatinib from the early post-transplant period was needed to effectively prevent BO.

### **Bone marrow-derived progenitor cells contributed to BO**

To determine the origin of the fibroblasts in the BO model, we used GFP-Tg mice as recipients of the tracheal allografts or as donors of the tracheal grafts (Figure 2). When BALB/c tracheal grafts were ectopically transplanted into GFP-Tg mice, the cells that accumulated in the oblitative lesions at 28 days were GFP-positive (Figure 2A). On the other hand, when GFP-Tg-derived grafts were transplanted

into BALB/c mice, the cells that accumulated in the obliterative lesion were GFP-negative (Figure 2B), indicating that the migrated cells that caused tracheal stenosis were of recipient origin. To determine to what extent BM-derived recipient cells contributed to the occlusion of the allograft, we used GFP-chimeric mice in which the original BM was replaced by GFP-marked BM cells. When BALB/c tracheal grafts were transplanted into GFP-chimeric mice,  $75.4 \pm 5.7\%$  of the cells in the obliterative area were GFP-positive (Figure 2C). The GFP-positive cells included round cells and spindle-shaped cells. The round cells were positive for CD45 (Figure 2D), indicating that they were inflammatory cells, such as macrophages and lymphocytes. The spindle-shaped cells were positive for collagen I (Figure 2E), indicating that they were mesenchymal cells, fibrocytes. These findings suggested that BM-derived fibrocytes contributed to the luminal obstruction in the BO model.

### **Imatinib reduced the number of fibrocytes *in vivo***

To clarify the effect of imatinib on fibrocytes *in vivo*, we determined the number of fibrocytes (CD45<sup>+</sup>/Pro-collagen I<sup>+</sup>) in each transplanted graft using immunofluorescent staining (Figure 3A). In all three groups, the number of infiltrating fibrocytes in the tracheal grafts gradually increased with time, peaked at day 7 and decreased thereafter. In the allografts obtained on days 3 and 7, the number of fibrocytes in the tracheal allograft of vehicle-treated recipients was significantly higher than those of the isograft. Imatinib administration significantly reduced the number of fibrocytes compared with vehicle (Figure 3B).

We next examined the three groups to determine the effect of imatinib on the accumulation of inflammatory cells in the transplanted graft after 7 days (Figure 3C). The numbers of inflammatory cells were all elevated in the tracheal allograft compared with those of the isograft. Unlike the number of fibrocytes, there were no significant differences in these inflammatory cell numbers between vehicle- and imatinib-treated allografts. Likewise, imatinib treatment did not affect the number of PECAM-1<sup>+</sup> endothelial cells or NG2<sup>+</sup> pericytes.

We examined murine fibrocytes for their expression of target proteins of imatinib. After 5 days of culturing murine PBMCs, we obtained spindle-shaped cells (fibrocytes) that co-expressed CD45 and procollagen I. Fibrocytes expressed high levels of c-Abl and PDGFR $\beta$  and low levels of c-Kit. These data indicated that c-Abl and PDGFR $\beta$  may be molecular targets for imatinib treatment (Figure 4).

### **Imatinib inhibited fibrocyte migration and differentiation *in vitro***

Fibrocytes originate from CD14<sup>+</sup> circulating blood mononuclear cells (a subpopulation of monocytes) (15, 29, 30). After 7 days of culturing human CD14<sup>+</sup> monocytes in serum-containing medium, we observed spindle-shaped cells, namely, fibrocytes; over 85% of the cells were double positive for CD45 and collagen I (Figure 5A). We first examined the expression of target proteins of imatinib on the surface of human CD14<sup>+</sup> monocytes and fibrocytes. Monocytes were positive for c-Abl and c-Kit, but negative for PDGFR (Figure 5B). This phenotype of monocytes was distinctly different from that of fibrocytes that were positive for c-Abl, PDGFR- $\beta$ , and c-Kit, but negative for PDGFR- $\alpha$ .

We assessed the effects of different cytokines on the migration of fibrocytes using Boyden chambers. PDGF-BB induced strong migration, whereas PDGF-AA and SCF did not (Figure 5C). PDGF-BB-induced migration of fibrocytes was significantly inhibited by imatinib treatment in a dose-dependent manner (Figure 5D), indicating that imatinib suppressed fibrocyte migration via the PDGF-PDGFR $\beta$  axis.

To analyze the effect of imatinib on the differentiation of fibrocytes, PBMCs were cultured in serum-free medium. After 5 days of culture, we observed the appearance of spindle-shaped cells, fibrocytes (Figure 6). Imatinib treatment reduced fibrocytes on day 5 in a dose-dependent manner, indicating that imatinib inhibited the differentiation of fibrocytes from CD14<sup>+</sup> monocytes (Figure 6A, B). Among other tyrosine kinase inhibitors including nilotinib, crenolanib, and masitinib, only nilotinib significantly inhibited differentiation of fibrocytes compared with controls (Figure 6C, D, E). Since nilotinib is more potent than imatinib in inhibiting activity of c-Abl tyrosine kinase (31, 32), c-Abl activity may be a possible candidate for regulating the differentiation into fibrocytes.

Finally, we used siRNA for c-Abl to determine if c-Abl could affect fibrocyte differentiation from CD14<sup>+</sup> monocytes. PBMCs that were transfected with 25 nM or 50 nM siRNA showed significantly less differentiation of fibrocytes compared with non-specific siRNA-transfected controls (Figure 6F, G). These findings indicated that imatinib might inhibit fibrocyte induction from CD14<sup>+</sup> monocytes via suppression of c-Abl of monocytes.

## DISCUSSION

Our study demonstrated that most of the accumulated mesenchymal cells in the tracheal allograft were of BM origin, and that imatinib ameliorated luminal occlusion by reducing the number of fibrocytes in the murine BO model. Moreover, imatinib inhibited fibrocyte migration as well as the differentiation of CD14<sup>+</sup> monocytes into fibrocytes *in vitro*, likely via the specific inhibition of c-Abl signaling.

Fibroblasts are generated from a variety of cell sources including resident mesenchymal cells, epithelial and endothelial cells, as well as BM-derived progenitor cells called fibrocytes (33-37). Mesenchymal stem cells are also associated with the pathogenesis of BO (38). It remains to be determined which cell sources are associated with the fibrogenesis of BO. Using a rat model, Sato et al. demonstrated that myofibroblasts in lung allografts were of extrapulmonary origin (39). However, the study did not determine whether the fibroblasts were derived from BM cell fibrocytes or surrounding mesenchymal cells. To address this issue, we established GFP chimeric mice to identify the origin of fibroblast-like cells. Our study indicated that fibrocytes participate in the fibrogenesis of BO in the HTT model.

The HTT model consists of an airway injury phase (days 1-3), an early inflammatory phase (days 3-14) and a late fibroproliferative phase (days 14-28). The mechanism responsible for the anti-fibrotic effect of imatinib was thought to be the inhibition of the early inflammatory phase because late administration of imatinib failed to exert anti-fibrotic effects. Moreover, imatinib administration reduced the fibrocyte counts in the tracheal allograft in the early inflammatory phase of the HTT model.

Based on our results, although the differences between the mouse model and human disease should be considered, prophylactic administration of imatinib is recommended for the treatment of BO.

Our study demonstrated for the first time that imatinib inhibited the differentiation of fibrocytes from CD14<sup>+</sup> monocytes by inhibiting c-Abl tyrosine kinase signaling. c-Abl is a non-receptor tyrosine kinase protein that regulates cellular proliferation and cytoskeletal remodeling (40). c-Abl is also involved in the differentiation of diverse cell types, including adipocytes, osteoblasts, and dendritic cells (41-43). The results of our study suggest that c-Abl tyrosine kinase signaling may play an important role in the differentiation of CD14<sup>+</sup> monocytes into fibrocytes.

Imatinib inhibits both migration and differentiation of fibrocytes *in vitro*; however, it is unknown which occurs predominantly *in vivo*. Previous animal studies suggest that differentiation of fibrocytes from circulating monocytes mainly occurs at tissue sites and not in the peripheral blood (17, 44, 45). A recent study demonstrated that the monocyte-macrophage axis contributed to the development of chronic graft-versus-host disease, including BO (46). In our HTT model, a larger number of monocytes accumulated in the tracheal allograft than the isograft, which may trigger graft rejection (47, 48). Therefore, imatinib may have mainly inhibited the differentiation of fibrocytes from monocytes in the transplanted graft rather than inhibiting the migration of circulating fibrocytes.

There are several limitations in our study. The murine trachea is anatomically different from the bronchiole in humans. In addition, neither hemoperfusion nor ventilation occurs in this HTT model. Finally, the tracheal obstruction in this model develops within one month compared with years in

transplanted human lungs (49). Although there are other BO models including an orthotopic tracheal or lung transplant system, these models are technically more challenging and represent a relatively earlier stage of bronchiolitis than the HTT model (49). Because the HTT model mimics the allo-immune pathological process of BO, it is useful for evaluating the pathogenetic role of fibrocytes in the development of BO.

In conclusion, imatinib could be potentially useful in preventing BO in lung transplant recipients. Our study also provides evidence that imatinib impairs fibrocyte differentiation by inhibiting c-Abl signaling *in vitro*. Another possible treatment of choice may be nilotinib, which has more potent and selective effects on c-Abl than imatinib and may therefore exert more beneficial effects on the suppression of BO. Further understanding of the potential roles of fibrocytes in the development of BO may help to develop effective biomarkers and novel anti-fibrotic therapy.

**Disclosures, funding, and acknowledgements:**

The authors have no conflicts of interest to disclose. The work was supported by JSPS KAKENHI Grant Numbers 23790901, 25860639, and 26931060.

The authors gratefully acknowledge Atsuo Kasada for sharing bone-marrow transplantation techniques, Hiroshi Kawasaki for providing experimental technique of immunofluorescence, Yuko Yamada for providing technique of immunohistochemistry, and Miki Kashiwano for experimental assistance.



## REFERENCES

1. Barker AF, Bergeron A, Rom WN, Hertz MI: Obliterative bronchiolitis. *N Engl J Med* 2014;370:1820-8.
2. Finlen Copeland CA, Snyder LD, Zaas DW, Turbyfill WJ, Davis WA, Palmer SM: Survival after bronchiolitis obliterans syndrome among bilateral lung transplant recipients. *Am J Respir Crit Care Med* 2010;182:784-9.
3. Carroll M, Ohno-Jones S, Tamura S, et al.: CGP 57148, a tyrosine kinase inhibitor, inhibits the growth of cells expressing BCR-ABL, TEL-ABL, and TEL-PDGFR fusion proteins. *Blood* 1997;90:4947-52.
4. Andrae J, Gallini R, Betsholtz C: Role of platelet-derived growth factors in physiology and medicine. *Genes Dev* 2008;22:1276-312.
5. Sadanaga A, Nakashima H, Masutani K, et al.: Amelioration of autoimmune nephritis by imatinib in MRL/lpr mice. *Arthritis Rheum* 2005;52:3987-96.
6. Schermuly RT, Dony E, Ghofrani HA, et al.: Reversal of experimental pulmonary hypertension by PDGF inhibition. *J Clin Invest* 2005;115:2811-21.
7. Daniels CE, Wilkes MC, Edens M, et al.: Imatinib mesylate inhibits the profibrogenic activity of TGF-beta and prevents bleomycin-mediated lung fibrosis. *J Clin*

Invest 2004;114:1308-16.

8. Aono Y, Nishioka Y, Inayama M, et al.: Imatinib as a novel antifibrotic agent in bleomycin-induced pulmonary fibrosis in mice. *Am J Respir Crit Care Med* 2005;171:1279-85.
9. Watanabe S, Waseda Y, Kimura H, et al.: Imatinib for bronchiolitis obliterans after allogeneic hematopoietic stem cell transplantation. *Bone Marrow Transplant* 2015;50:1250-2.
10. Magro L, Mohty M, Catteau B, et al.: Imatinib mesylate as salvage therapy for refractory sclerotic chronic graft-versus-host disease. *Blood* 2009;114:719-22.
11. Olivieri A, Locatelli F, Zecca M, et al.: Imatinib for refractory chronic graft-versus-host disease with fibrotic features. *Blood* 2009;114:709-18.
12. Olivieri A, Cimminiello M, Corradini P, et al.: Long-term outcome and prospective validation of NIH response criteria in 39 patients receiving imatinib for steroid-refractory chronic GVHD. *Blood* 2013;122:4111-8.
13. Kallio EA, Koskinen PK, Aavik E, Buchdunger E, Lemstrom KB: Role of platelet-derived growth factor in obliterative bronchiolitis (chronic rejection) in the rat. *Am J Respir Crit Care Med* 1999;160:1324-32.
14. Tikkanen JM, Hollmen M, Nykanen AI, Wood J, Koskinen PK, Lemstrom KB: Role of platelet-derived growth factor and vascular endothelial growth factor in obliterative airway disease. *Am J Respir Crit Care Med* 2006;174:1145-52.
15. Reilkoff RA, Bucala R, Herzog EL: Fibrocytes: emerging effector cells in chronic inflammation. *Nat Rev Immunol* 2011;11:427-35.
16. Moeller A, Gilpin SE, Ask K, et al.: Circulating fibrocytes are an indicator of poor prognosis in idiopathic pulmonary fibrosis. *Am J Respir Crit Care Med* 2009;179:588-94.
17. Haudek SB, Xia Y, Huebener P, et al.: Bone marrow-derived fibroblast precursors mediate ischemic cardiomyopathy in mice. *Proc Natl Acad Sci U S A* 2006;103:18284-9.
18. Kisseleva T, Uchinami H, Feirt N, et al.: Bone marrow-derived fibrocytes participate in pathogenesis of liver fibrosis. *J Hepatol* 2006;45:429-38.
19. Andersson-Sjoland A, Erjefalt JS, Bjermer L, Eriksson L, Westergren-Thorsson G: Fibrocytes are associated with vascular and parenchymal remodelling in patients with obliterative bronchiolitis. *Respir Res* 2009;10:103.
20. LaPar DJ, Burdick MD, Emamina A, et al.: Circulating fibrocytes correlate with bronchiolitis obliterans syndrome development after lung transplantation: a novel clinical biomarker. *Ann Thorac Surg* 2011;92:470-7; discussion 7.
21. Hertz MI, Jessurun J, King MB, Savik SK, Murray JJ: Reproduction of the obliterative bronchiolitis lesion after heterotopic transplantation of mouse airways. *Am J Pathol* 1993;142:1945-51.
22. Jungraithmayr W, Jang JH, Schrepfer S, Inci I, Weder W: Small animal models

- of experimental obliterative bronchiolitis. *Am J Respir Cell Mol Biol* 2013;48:675-84.
23. Hashimoto N, Jin H, Liu T, Chensue SW, Phan SH: Bone marrow-derived progenitor cells in pulmonary fibrosis. *J Clin Invest* 2004;113:243-52.
  24. Shao DD, Suresh R, Vakil V, Gomer RH, Pilling D: Pivotal Advance: Th-1 cytokines inhibit, and Th-2 cytokines promote fibrocyte differentiation. *J Leukoc Biol* 2008;83:1323-33.
  25. Curnow SJ, Fairclough M, Schmutz C, et al.: Distinct types of fibrocyte can differentiate from mononuclear cells in the presence and absence of serum. *PLoS One* 2010;5:e9730.
  26. Garcia-de-Alba C, Becerril C, Ruiz V, et al.: Expression of matrix metalloproteases by fibrocytes: possible role in migration and homing. *Am J Respir Crit Care Med* 2010;182:1144-52.
  27. Aono Y, Kishi M, Yokota Y, et al.: Role of platelet-derived growth factor/platelet-derived growth factor receptor axis in the trafficking of circulating fibrocytes in pulmonary fibrosis. *Am J Respir Cell Mol Biol* 2014;51:793-801.
  28. Pilling D, Vakil V, Gomer RH: Improved serum-free culture conditions for the differentiation of human and murine fibrocytes. *J Immunol Methods* 2009;351:62-70.
  29. Abe R, Donnelly SC, Peng T, Bucala R, Metz CN: Peripheral blood fibrocytes: differentiation pathway and migration to wound sites. *J Immunol* 2001;166:7556-62.
  30. Bellini A, Mattoli S: The role of the fibrocyte, a bone marrow-derived mesenchymal progenitor, in reactive and reparative fibroses. *Lab Invest* 2007;87:858-70.
  31. Weisberg E, Manley P, Mestan J, Cowan-Jacob S, Ray A, Griffin JD: AMN107 (nilotinib): a novel and selective inhibitor of BCR-ABL. *Br J Cancer* 2006;94:1765-9.
  32. O'Hare T, Walters DK, Stoffregen EP, et al.: In vitro activity of Bcr-Abl inhibitors AMN107 and BMS-354825 against clinically relevant imatinib-resistant Abl kinase domain mutants. *Cancer Res* 2005;65:4500-5.
  33. Brazelton TR, Shorthouse R, Huang X, Morris RE: Infiltrating recipient mesenchymal cells form the obliterative airway disease lesion and dramatically remodel graft tissue in a model of chronic lung rejection. *Transplant Proc* 1997;29:2614.
  34. Brocker V, Langer F, Fellous TG, et al.: Fibroblasts of recipient origin contribute to bronchiolitis obliterans in human lung transplants. *Am J Respir Crit Care Med* 2006;173:1276-82.
  35. Yousem SA, Sherer C, Fuhrer K, Cieply K: Myofibroblasts of recipient origin are not the predominant mesenchymal cell in bronchiolitis obliterans in lung allografts. *J Heart Lung Transplant* 2013;32:266-8.
  36. Lama VN, Phan SH: The extrapulmonary origin of fibroblasts: stem/progenitor cells and beyond. *Proc Am Thorac Soc* 2006;3:373-6.
  37. Wynn TA: Cellular and molecular mechanisms of fibrosis. *J Pathol* 2008;214:199-

210.

38. Salama M, Andrukhova O, Jaksch P, et al.: Endothelin-1 governs proliferation and migration of bronchoalveolar lavage-derived lung mesenchymal stem cells in bronchiolitis obliterans syndrome. *Transplantation* 2011;92:155-62.
39. Sato M, Hirayama S, Lara-Guerra H, et al.: MMP-dependent migration of extrapulmonary myofibroblast progenitors contributing to posttransplant airway fibrosis in the lung. *Am J Transplant* 2009;9:1027-36.
40. Sirvent A, Benistant C, Roche S: Cytoplasmic signalling by the c-Abl tyrosine kinase in normal and cancer cells. *Biol Cell* 2008;100:617-31.
41. Appel S, Rupf A, Weck MM, et al.: Effects of imatinib on monocyte-derived dendritic cells are mediated by inhibition of nuclear factor-kappaB and Akt signaling pathways. *Clin Cancer Res* 2005;11:1928-40.
42. Lee YC, Huang CF, Murshed M, et al.: Src family kinase/abl inhibitor dasatinib suppresses proliferation and enhances differentiation of osteoblasts. *Oncogene* 2010;29:3196-207.
43. Keshet R, Bryansker Kraitshstein Z, Shanzer M, Adler J, Reuven N, Shaul Y: c-Abl tyrosine kinase promotes adipocyte differentiation by targeting PPAR-gamma 2. *Proc Natl Acad Sci U S A* 2014;111:16365-70.
44. Frid MG, Brunetti JA, Burke DL, et al.: Hypoxia-induced pulmonary vascular remodeling requires recruitment of circulating mesenchymal precursors of a monocyte/macrophage lineage. *Am J Pathol* 2006;168:659-69.
45. Varcoe RL, Mikhail M, Guiffre AK, et al.: The role of the fibrocyte in intimal hyperplasia. *Journal of thrombosis and haemostasis : JTH* 2006;4:1125-33.
46. Alexander KA, Flynn R, Lineburg KE, et al.: CSF-1-dependant donor-derived macrophages mediate chronic graft-versus-host disease. *J Clin Invest* 2014;124:4266-80.
47. Zecher D, van Rooijen N, Rothstein DM, Shlomchik WD, Lakkis FG: An innate response to allogeneic nonself mediated by monocytes. *J Immunol* 2009;183:7810-6.
48. Oberbarnscheidt MH, Zeng Q, Li Q, et al.: Non-self recognition by monocytes initiates allograft rejection. *J Clin Invest* 2014;124:3579-89.
49. Fan K, Qiao XW, Nie J, et al.: Orthotopic and heterotopic tracheal transplantation model in studying obliterative bronchiolitis. *Transpl Immunol* 2013;28:170-5.

## Figure Legends

**Figure 1.** Morphological features of murine bronchiolitis obliterans (BO) after heterotopic tracheal transplantation. (A) Representative images of hematoxylin and eosin (H&E) staining of tracheal isograft and allograft tissue on days 7, 14, and 28. Insets in each image show a high power field of airway lesion. *Scale bar* = 100  $\mu\text{m}$ . (B) Quantitative morphometric analysis of airway injury and luminal occlusion in isograft and allograft. Data represent the means  $\pm$  SEM.  $n = 6 - 8/\text{group}$ . \*,  $P < 0.05$  for allograft compared with isograft. (C) Representative H&E stained sections of vehicle-treated tracheal allograft (Vehicle), imatinib-treated tracheal allograft on days 1 through 28 (Prophylaxis), on days 1 through 14 (Early treatment), and on days 15 through 28 (Late treatment) after transplantation. *Scale bar* = 100  $\mu\text{m}$ .

(D) Quantitative morphometric analysis of airway injury and luminal occlusion in each group. Data represent the means  $\pm$  SEM. n = 6 - 8/group. \*,  $P < 0.05$ .

**Figure 2.** Immunohistochemical staining of Green fluorescent protein (GFP) in allograft tissue sections 28 days after transplantation. (A-C) Representative images of GFP immunohistochemical stains in BALB/c tracheas transplanted to GFP-transgenic mice (A), GFP-transgenic mouse tracheas transplanted to BALB/c mice (B), and BALB/c tracheas transplanted to C57BL/6 wild-type mice treated with GFP-transgenic BM transplantation (C). High power field of obliterative area is shown enlarged below each image. Brown stain indicates GFP-positive cells. All sections are counterstained lightly with hematoxylin to visualize negatively stained cells. *Scale bars* = 50  $\mu$ m. (D and E) Representative images of immunofluorescent staining of BALB/c tracheas transplanted to C57BL/6 wild-type mice treated with GFP-transgenic BM transplantation. GFP-positive cells (green) are also positive for CD45 (red) (D) and collagen-I (red) (E). *Scale bar* = 20  $\mu$ m.

**Figure 3.** Fibrocytes, inflammatory cells and vessel markers in transplanted tracheal grafts. (A) Representative image of immunofluorescence staining with anti-CD45 (green), anti-pro-collagen I (red) antibodies, and Hoechst 33342 (blue) in vehicle- and imatinib-treated allograft. Double-positive cells expressing CD45 and pro-collagen I are fibrocytes (*arrows*). *Scale bar* = 20  $\mu$ m. (B) Time course showing the number of fibrocytes in an isograft, and vehicle- and imatinib-treated allografts. Data

represent the means  $\pm$  SEM. n = 4/group. \*,  $P < 0.05$  for vehicle-treated allograft compared with isograft. \*\*,  $P < 0.05$  for imatinib-treated compared with vehicle-treated allograft. (C) Inflammatory cells included monocytes (CD11b), macrophages (F4/80), T lymphocytes (CD3) and neutrophils (MPO). Vessel markers included endothelial cells (PECAM-1) and pericytes (NG2). Data represent the means  $\pm$  SEM. n = 4/group. \*,  $P < 0.05$ . NS = not significant; Vehicle = vehicle-treated allograft; Imatinib = imatinib-treated allograft.

**Figure 4.** Protein expression in murine fibrocytes. (A) Representative images of cells immunostained for pro-collagen I (red), CD45 (green) and Hoechst 33342 (blue) in cultured murine fibrocytes. (B) Representative images showing cells immunostained for c-Abl, PDGFR $\alpha$ , PDGFR $\beta$ , and c-Kit (red). *Scale bar = 20  $\mu$ m.*

**Figure 5.** Protein expression by human fibrocytes and their migration. (A) Representative image of fibrocytes after 8 days of cultivation of human blood monocytes. *Scale bar = 100  $\mu$ m.* Fibrocytes were over 90% pure as determined by flow cytometric analysis using anti-CD45 and anti-collagen I antibodies. (B) Protein expression by human monocytes and fibrocytes assessed by flow cytometry. The analyzed proteins included CD14 (monocyte marker), collagen I (mesenchymal marker), c-Abl, PDGFR- $\alpha$ , PDGFR- $\beta$ , and c-Kit. Representative experiments are shown in red, with isotype controls shown in gray shades. (C) Effect of chemotactic factors on fibrocyte migration assessed by using

Boyden-chamber assays. The cells that migrated to the lower side of the membrane were counted and expressed as a percentage of total cells. The data represent means  $\pm$  SEM of 3 independent experiments.

\*,  $P < 0.05$ . (D) Effect of imatinib on PDGF-BB-enhanced migration of fibrocytes. The data represents means  $\pm$  SEM of 3 independent experiments. \*,  $P < 0.05$ .

**Figure 6.** Imatinib inhibited fibrocyte differentiation. (A) Representative image of cultured fibrocytes.

Peripheral blood mononuclear cells (PBMCs) were cultured in serum-free medium for 5 days in the presence or absence of imatinib. Some PBMCs became spindle-shaped fibrocytes (arrow). *Scale bar =*

100  $\mu$ m. (B) The number of fibrocytes was assessed after 5 days of culture and expressed as a percentage

of total cells. (C-E) PBMCs treated with other inhibitors including nilotinib, crenolanib, and masitinib.

The number of fibrocytes was evaluated after 5 days of culture. The data represent means  $\pm$  SEM of 3

independent experiments. (F) Knockdown of c-Abl inhibited the differentiation of fibrocytes 48 h after

incubation. Flow cytometric analysis of c-Abl protein in cultured-fibrocytes after siRNA transfection.

Black-filled histograms show the cultured-fibrocytes in the presence of 50 nM c-Abl siRNA, gray-

shaded histograms show results from treatment with control siRNA, and white histograms show isotype

control (G) The siRNA knockdown of c-Abl significantly decreased the number of fibrocytes compared

with siRNA-free controls. The data represent mean  $\pm$  SEM of 3 independent experiments. \*,  $P < 0.05$ .





Figure 1

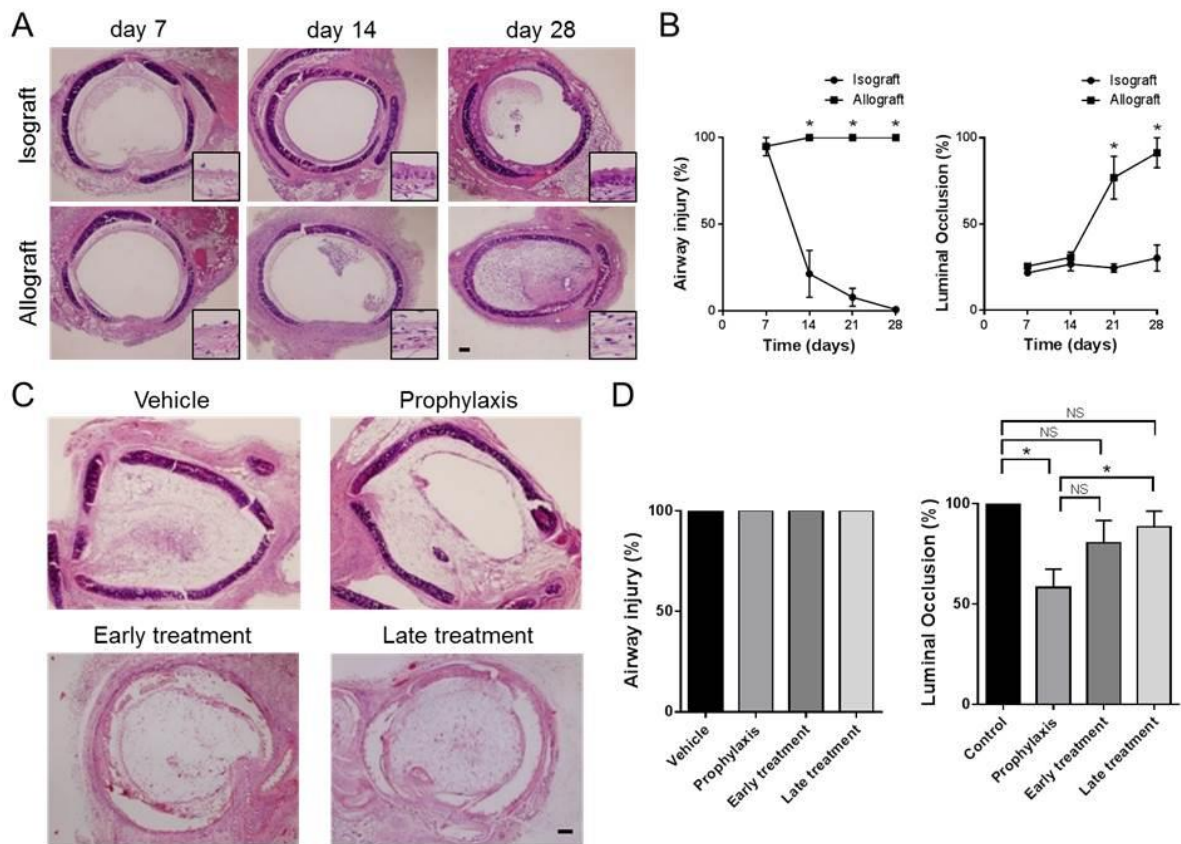


Figure 2

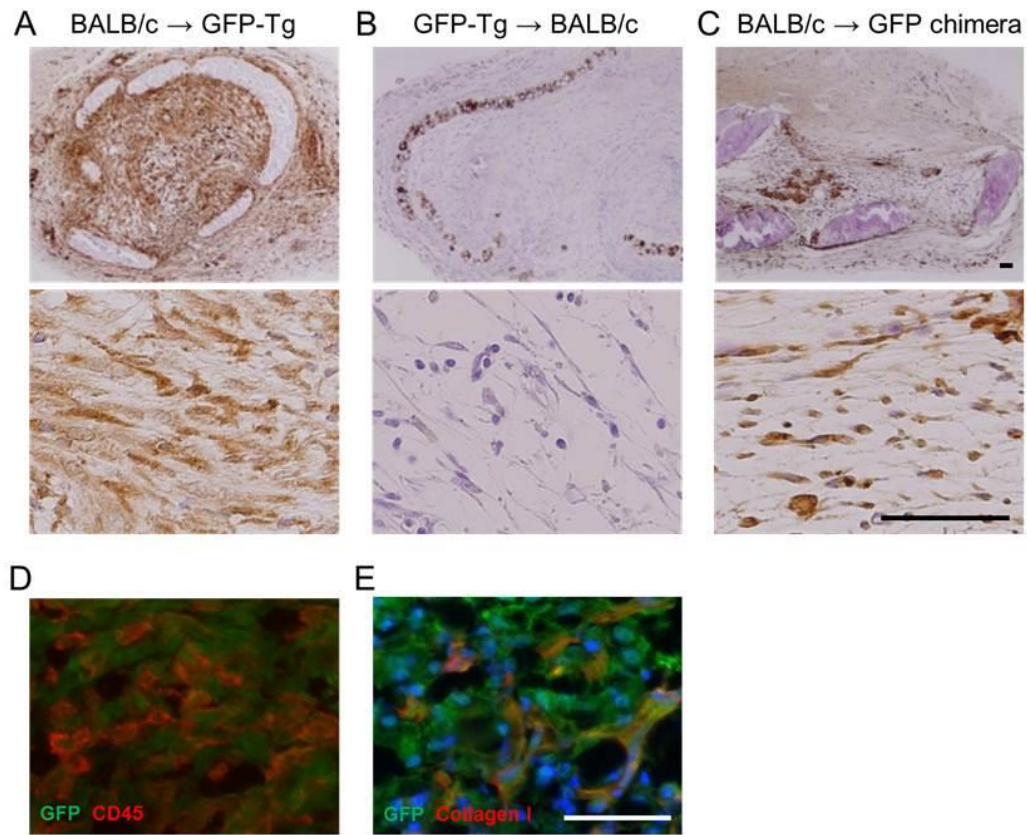


Figure 3

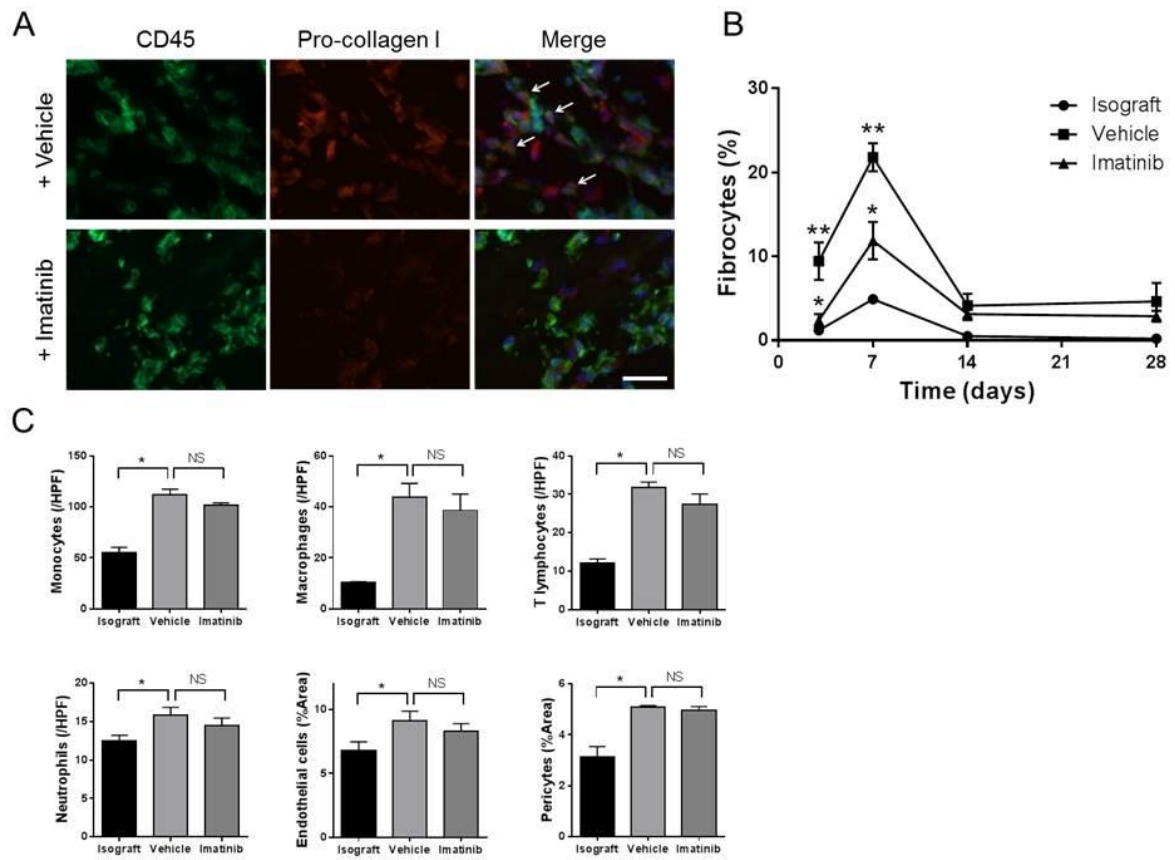


Figure 4

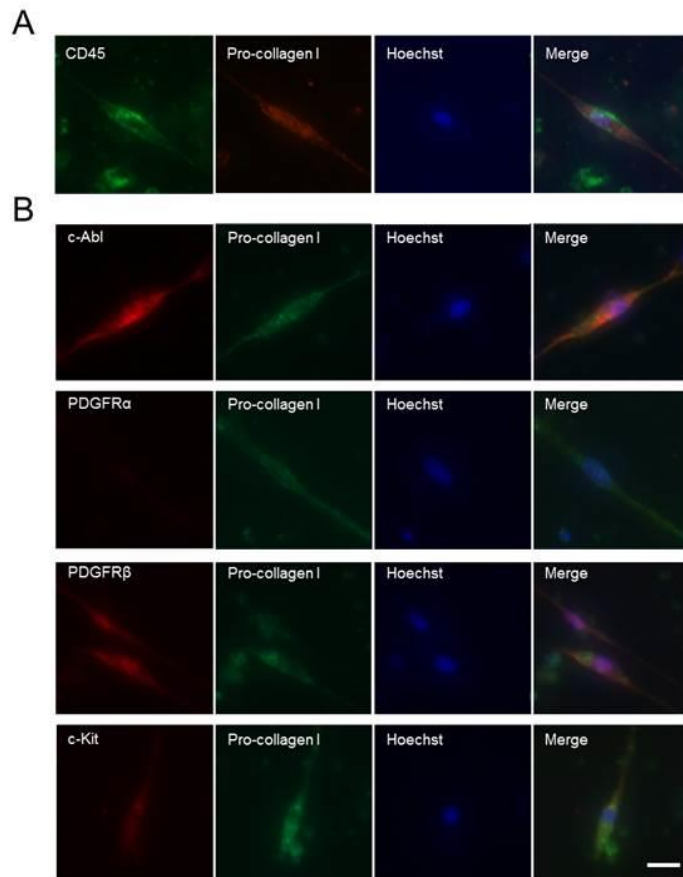


Figure 5

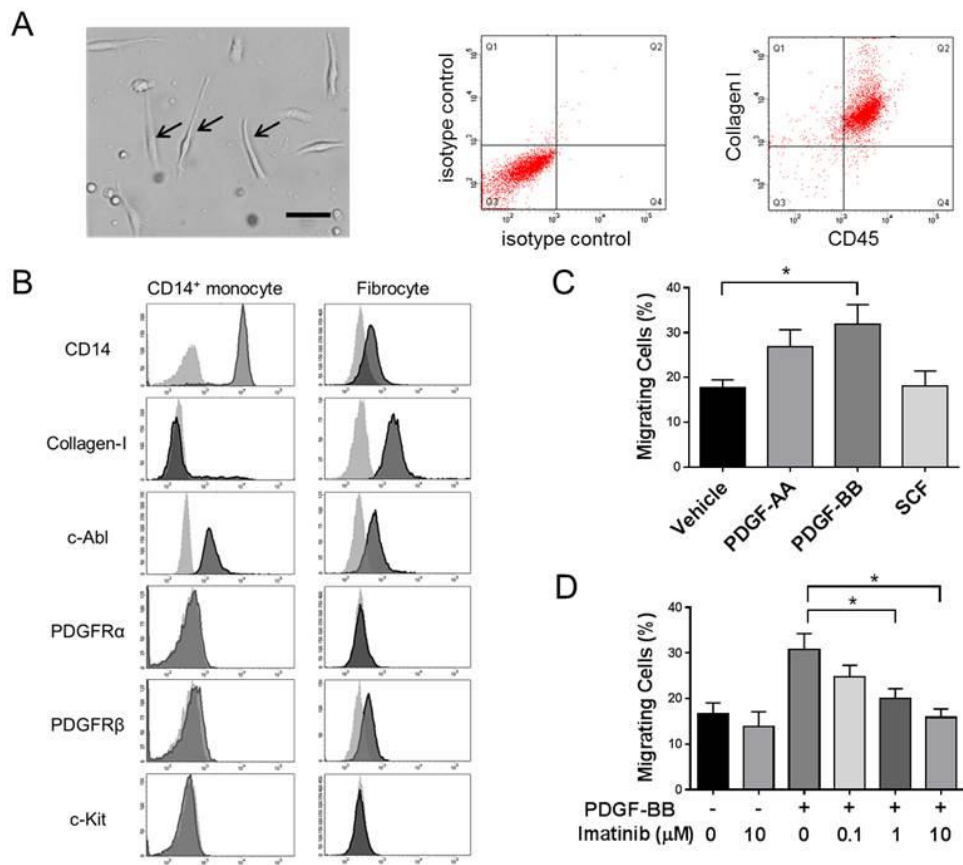


Figure 6

